



Development of a tumor tissue-mimicking model with endothelial cell layer and collagen gel for evaluating drug penetration



Noboru Sasaki^{a,*}, Clemens Bos^a, Jean-Michel Escoffre^a, Gert Storm^{b,c}, Chrit Moonen^a

^a Imaging Division, University Medical Center Utrecht, Utrecht, The Netherlands

^b Department of Pharmaceutics, Utrecht Institute of Pharmaceutical Sciences, Utrecht University, Utrecht, The Netherlands

^c Department Biomaterials Science & Technology (BSTO), Section Targeted Therapeutics, MIRA – Institute for Biomedical Technology and Technical Medicine, University of Twente, The Netherlands

ARTICLE INFO

Article history:

Available online 21 January 2015

Keywords:

Drug penetration
Endothelial layer
Extracellular matrix
Tissue-mimicking model

ABSTRACT

The endothelial cells of vessels, the interstitial matrix and the distance between the tumor cells and vessels, are the major penetration barriers for intravenously administered anticancer drugs in reaching tumor cells after intravenous injection. The availability of a tumor tissue-mimicking model that includes both the endothelial cell layer and the extracellular matrix would be beneficial to assess drug penetration in early stages of drug development. Here, we propose a novel *in vitro* model for studying the above mentioned barriers. Human umbilical vein endothelial cells were cultured as a single layer on a collagen type-I coated permeable cell culture insert. After culturing for five days, the insert was superimposed on collagen type-I gel containing cancer cells. The system was evaluated for assessing penetration-enhancement by ultrasound triggered microbubble cavitation. Our model allowed visualization of the penetration distance of a model drug (fluorescein isothiocyanate – Dextran 500000-conjugated, FD500) from the endothelial cell layer into the cancer cell containing collagen matrix upon different sonication treatments. Initial results showed that the model allows the visualization of drug penetration and that the endothelial cell layer is affecting this. The presented *in vitro* model aims to mimic vessels and stromal tissue in cancer, and thus can aid in the assessment of drug penetration in the case of tumor-targeted drug delivery, and in the reduction and refinement of animal studies.

© 2015 Published by Elsevier B.V.

1. Introduction

Efficient drug penetration in tumor tissue is an important goal in anticancer drug development. Because the majority of anticancer drugs has to reach the target tumor cells *via* the circulation, the distance between the cells and the nearest vessels is a critical factor determining the drug delivery to the tumor cells. The abnormal vascularity in solid tumors often leads to relatively long distances from endothelial linings to tumor cells. In addition, increased interstitial fluid pressure and the extracellular matrix (ECM) are potential penetration-limiting factors to be taken into account (Minchinton and Tannock, 2006). Real-time imaging with an intravital or a multi-photon microscope (Manzoor et al., 2012; Nhan et al., 2013) and histological analysis of tumor sections (Kyle et al., 2007; Primeau et al., 2005) are direct methods to assess drug

penetration into tumor tissue. However, because of the heterogeneity of cancer tissues, it is difficult to quantitatively and objectively assess the drug penetration characteristics. Moreover, such *in vivo* experiments call for extensive use of laboratory animals. Thus, the availability of a three-dimensional (3D) tumor tissue mimicking *in vitro* model would be useful and ethically desirable. Multicellular spheroid and multilayered cell cultures are the major cell-based *in vitro* systems to evaluate drug penetration (Grainger et al., 2010; Ingargiola et al., 2014; Kyle et al., 2004; Sagnella et al., 2014). Even though these culture methods are superior to the conventional single tumor cell layer culture method, they still lack some characteristics that are critical. Firstly, the vascular wall, in particular the endothelial cell layer, is the first physical barrier for systemically administered anticancer drugs. Secondly, without the endothelial cell layer, the penetration distance beyond this barrier cannot be assessed. Thirdly, the ECM in cancer stroma has a great impact on cancer chemotherapy (McMillin et al., 2013), and a tissue mimicking system should preferably also allow the presence of an ECM. It is known that poorly curable cancer is often stroma-rich (Nishihara, 2014). Therefore, an *in vivo* “tumor tissue” culture system including

* Corresponding author at: Imaging Division, University Medical Center Utrecht, Heidelberglaan 100, 3584 CX, Utrecht, The Netherlands. Tel.: +31 0 887569665; fax: +31 0 887555850.

E-mail address: n.sasaki@umcutrecht.nl (N. Sasaki).

tumor cells, the endothelial cell layer and ECM may provide a realistic *in vivo* mimicking model that will allow to study aspects of *in vivo* drug penetration more precisely.

Here we propose an *in vitro* model for evaluating drug penetration into tumor tissue. It is composed of two compartments: a single layer of endothelial cells and a collagen type-I matrix containing cancer cells. Our model allows visualization of the diffusion distance from the endothelial cell layer in an ECM-rich 3D structure along with the integrity of the endothelial cell layer. In this study, we choose ultrasound-triggered microbubble cavitation as the drug delivery enhancement method (Lentacker et al., 2014) to demonstrate the suitability of the proposed system for evaluating drug penetration in tumor tissue. Because microbubbles remain inside vessels, the impact of the endothelial cell layer on drug penetration was assessed. Here we show our preliminary results, obtained with the model drug fluorescein isothiocyanate – Dextran 500000-conjugated (FD500), suggesting that the developed *in vitro* model is suitable for the evaluation of drug penetration in tumor tissue.

2. Material and methods

2.1. Tissue-mimicking model

The *in vitro* model for evaluating drug penetration into tumor tissue is outlined in Fig. 1.

2.1.1. The upper compartment

Human umbilical vein endothelial cells (HUVECs) were cultured in EBM-2 medium (Lonza Cologne GmbH, Germany) supplemented with SingleQuats kit (Lonza Cologne GmbH) and incubated at 37 °C in a humidified atmosphere with 5% CO₂. The medium was changed every second day. Cells were used at passage 5 or 6 in all experiments. In order to obtain a matured endothelial layer, cell culture inserts with transparent polyethylene terephthalate track-etched membrane (12 well format, 1.0 µm pore size, Corning BV, the Netherlands) were coated by collagen type-I (Collagen I High Concentration, Rat tail, Corning BV). Each insert was incubated with 10 µg collagen type-I in phosphate buffered solution (PBS) and a reconstruction buffer (50 mM NaOH, 260 mM NaHCO₃, 200 mM HEPES) for 1 h at room temperature. The membrane surface was rinsed once by PBS and the medium. Cells were seeded on the coated inserts at the density of 1.0×10^5 cells/insert and cultured for 5 days with daily medium change.

2.1.2. The lower compartment

In order to mimic the tumor tissue, cancer cells were embedded in the collagen-I gel. FaDu (human pharynx squamous cell

carcinoma, HTB-43[®]; ATCC, VA, USA) cells were cultured in Waymouth MB 732/1 medium (Sigma–Aldrich[®], the Netherlands) supplemented with 10% fetal bovine serum (Sigma–Aldrich[®]). Cells were kept in the humidified incubator and the medium was changed every three days. FaDu cell suspension was mixed with collagen-I solution that consists of 10× Waymouth MB 732/1 medium, the reconstruction buffer, additional 1 M NaOH (to adjust pH), and 10% FBS. A volume of 800 µL gel-cell solution, containing 0.8×10^6 FaDu cells, was added to the 12-well Companion plate (Corning BV) and was incubated for 30 min at 37 °C in a humidified atmosphere with 5% CO₂.

2.2. Model drug

Fluorescein isothiocyanate – Dextran 500000-conjugated (FD500; Sigma–Aldrich[®]) was used in this preliminary study, since its molecular weight, and thus also its diffusion distance is similar to many macromolecular drugs.

2.3. Ultrasound triggered microbubble cavitation

The insert with HUVECs was superimposed on the gel–cell layer after the incubation. Then, 0.5 mg/mL FD500 and 4 µL SonoVue (Bracco Research, Italy) were added to the insert. Thereafter, the plate was covered by Parafilm M[®] (Pechiney Plastic Packaging, IL, USA) and immediately inverted. In order to assure cell–bubble contact, the plate was kept inversed for 15 min at room temperature before ultrasound exposure.

Ultrasound was generated using a 5.8 mm-diameter mono-element transducer (Precision Acoustics, UK) driven by an electrical signal generated by an arbitrary waveform generator (Agilent 33120A, Malaysia), then amplified by a power amplifier (KMP Electronics, France). Ultrasound parameters were as follows; 1.3 MHz center frequency, 100 µs pulse width, 1 kHz pulse repetition frequency, 1.0 MPa peak-to-peak pressure, 30 s exposure. The acoustic pressure was measured using a calibrated 10 µm fiber-optic hydrophone (Precision Acoustics, UK). The acoustic pressure corresponds to a mechanical index of 0.44, which is not excessive (Choi et al., 2011) and is available using diagnostic ultrasound imaging modality (Carson et al., 2012; Hauff et al., 2005; Tinkov et al., 2010). The plate was incubated for an additional 15 min at room temperature after ultrasound exposure. The superimposed insert was removed and used for immunostaining or flow cytometric analysis. In order to minimize additional FD500 diffusion, the gel–cell layer was rinsed once by PBS right after the insert removal, immediately frozen in liquid nitrogen, and kept in liquid nitrogen until cryosectioning.

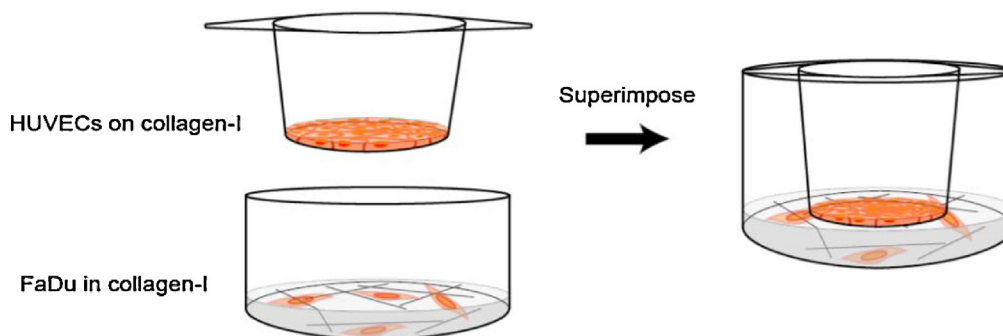


Fig. 1. Schematic illustration of the tissue-mimicking model. Human umbilical vein endothelial cells (HUVECs) are cultured on a collagen type-I (collagen-I) coated permeable insert for 5 days. When the HUVECs have grown to form a complete endothelial sheet, the insert with HUVECs is placed on the collagen-I gel containing cancer cells, in this case FaDu cells.

2.4. Characterization of the endothelial cell layer

2.4.1. Immunostaining

The endothelial cell layer in the insert was stained by CD31 (PECAM-1) or VE-cadherin (CD144) antibodies in order to observe the monolayer integrity. The cells were fixed with 4% paraformaldehyde in PBS for 10 min. Subsequently, cells were washed with PBS and permeabilized with 0.5% Triton X-100 in PBS for 15 min. After additional washing steps, the cells are incubated with 3% (w/v) bovine serum albumin in PBS for 1 h. Thereafter, the cells were incubated with rabbit polyclonal anti-CD31 antibody (1:20; Abcam, UK) for 4 h at room temperature, or rabbit polyclonal anti-VE Cadherin antibody (1:500; Abcam, UK) overnight at 4 °C. Cells were then washed and incubated in the dark for 30 min at room temperature with Alexa Fluor 568-conjugated goat anti-rabbit IgG (1:500; Life

Technologies Europe BV, The Netherlands). The integrity of the endothelial cell layer on the whole insert was observed by a fluorescence microscope, Keyence BZ-9000 (Keyence International, Belgium).

2.5. Cryosectioning and fluorescence measurement

The frozen gel layer was sectioned by CM 3050 (Leica Microsystems BV, the Netherlands) at 10 μ m thickness. Groups of five consecutive sections were put in the same well of a 48-well plate containing 100 μ L of 1% Triton X-100 in PBS and incubated at 45 °C for 40 min. The fluorescence intensity from the dissolved sections was measured by Fluorolog-3 (Horiba Scientific, Edison, NJ, USA). The excitation wavelength was 490 nm, and the emission wavelength was 520 nm.

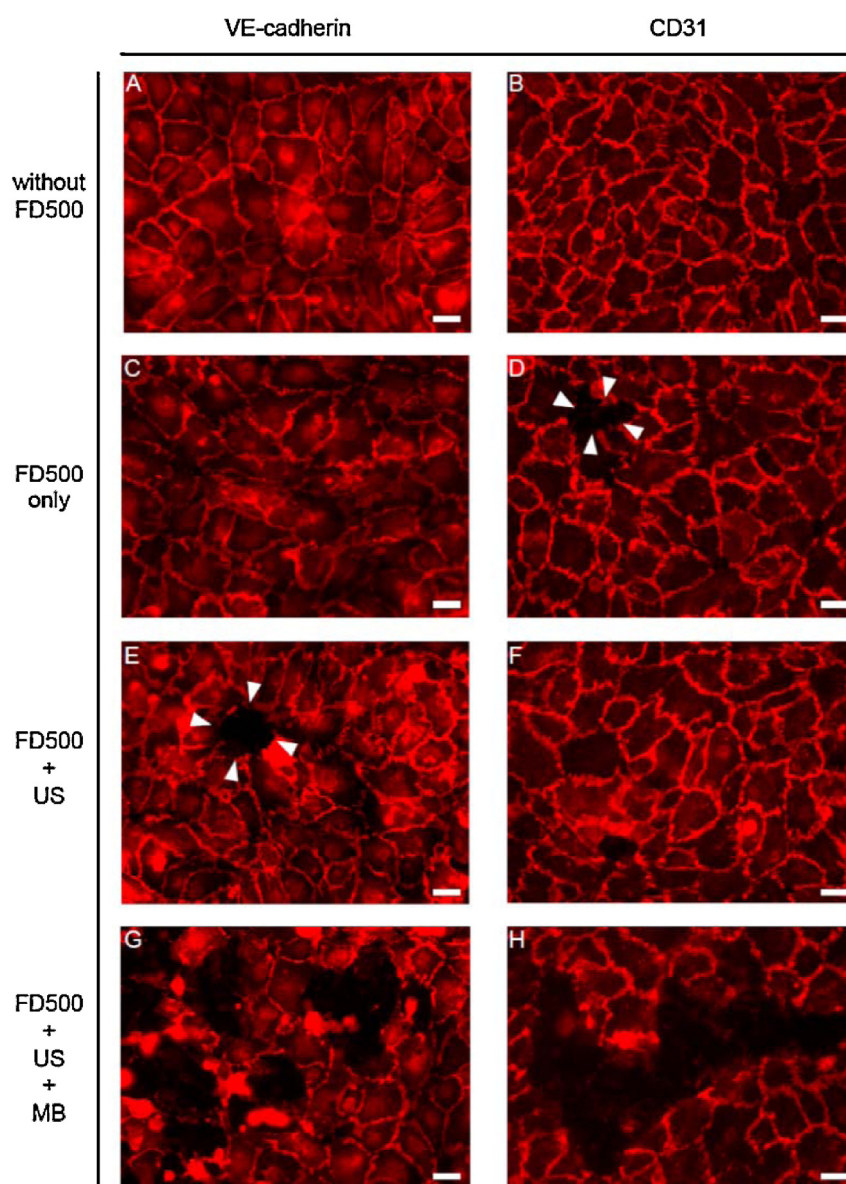


Fig. 2. Fluorescence images of the HUVEC monolayer. Immunostainings with CD31 (A, C, E, G) and VE-cadherin (B, D, F, H) antibodies are shown. Incubation with FD500 slightly damaged HUVECs (presence of small gaps, see arrow heads, D). Ultrasound (US) did not enhance the FD500-mediated cell damage (arrow heads in E; F). Addition of microbubbles (MB) induced cell detachment upon US exposure (G and H). Bars, 20 μ m.

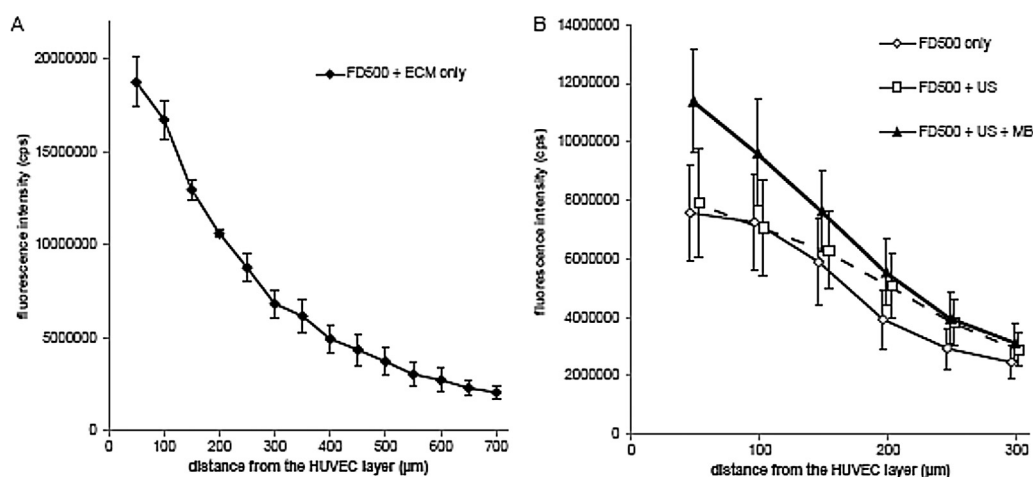


Fig. 3. Fluorescence intensity in the gel as a function of distance to the HUVEC layer. The fluorescence intensity of dissolved gel sections was measured to evaluate the diffusion distance of FD500 into the gel after different treatments. (A) Fluorescence intensity penetration into the gel without the presence of the HUVEC layer, (B) Fluorescence intensity penetration over an initial distance of 300 μm with the HUVEC layer present. The data represent the mean \pm standard error of the mean of five independent experiments. FD500 + ECM only, addition of FD500 to the insert without the HUVEC layer; FD500 only, addition of FD500 to the insert with the HUVEC layer; FD500 + US, addition of FD500 to the insert with the HUVEC layer followed by ultrasound exposure; FD500 + US + MB, addition of FD500 and microbubbles to the insert with the HUVEC layer followed by ultrasound exposure.

3. Results

3.1. The upper compartment: HUVEC layer (Fig. 2)

After 5 days of culturing HUVECs, an endothelial monolayer was formed on the insert membrane (Fig. 2A and B). Its integrity after different treatments is shown in Fig. 2: addition of FD500 (FD500 only), addition of FD500 followed by ultrasound exposure (FD500 + US), and addition of FD500 and microbubbles followed by ultrasound exposure (FD500 + US + MB). FD500 slightly damaged the HUVEC layer (Fig. 2C and D). Ultrasound did not enhance the minor damage (Fig. 2E and F). Addition of microbubbles generated a clear cell detachment upon US exposure (Fig. 2G and H).

3.2. The lower compartment: FD500 diffusion through the gel layer (Fig. 3)

Cryosectioning of the gel layer and fluorescence intensity measurement of sections were performed to evaluate the penetration of FD500 into the gel layer with a spatial resolution of 50 μm . Fig. 3A shows a fluorescence intensity vs. distance profile of FD500 in the gel layer without the HUVEC layer. Fig. 3B shows fluorescence intensity vs. distance profiles after the different treatments in the presence of the HUVEC layer. It can be observed that the presence of the endothelial cell layer (3B) decreased the peak fluorescence intensity. Addition of microbubbles and ultrasound led to a modest stimulatory effect on the degree of drug penetration relatively close to the HUVEC layer. Ultrasound alone did not have any effect on the penetration profile.

4. Conclusion and final remarks

This preliminary study shows the feasibility of our *in vitro* tumor-tissue mimicking model for evaluating drug penetration in solid tumor tissue. Our model visualized the penetration of FD500 along with the evaluation of the integrity and morphology of the endothelial cell layer. The results show the presence of the endothelial cell layer influenced the drug penetration into the collagen gel. Because the radius of FD500 is 14.7 nm, the intercellular pathway is likely the major route of passage through the endothelial cell layer of the model drug under the conditions of

this study (Komarova and Malik, 2010). The results of this preliminary study suggest that the treatment with microbubbles and ultrasound enhanced the permeability of the HUVEC layer mainly by inducing detachment of the HUVEC cells, which enhances the model drug penetration into the collagen gel relatively close to the HUVEC layer (up to about 50 μm). It must be noted that assessment of the influence of cavitation is not the primary objective of this report, but that we intend to illustrate in this preliminary study that the model used here can be useful for studying drug transport processes like extravasation and intratumoral penetration.

Author contributions

NS is responsible for the design of experiments, performance of all experiments, analysis of data and writing of the manuscript. JME and GS contributed to the writing of the manuscript. CM and CB are responsible for the reviewing of the manuscript and the supervision of this work.

Acknowledgments

The authors appreciate J.B. van den Dikkenberg, M.J. van Steenberg, and G. Nadibaidze (Department of Pharmaceutics, Utrecht Institute for Pharmaceutical Sciences, Utrecht University, The Netherlands) for their technical assistance. This work was supported by Advanced ERC grant Sound Pharma – 268906 (CM).

References

- Carson, A.R., McTiernan, C.F., Lavery, L., Grata, M., Leng, X., Wang, J., Chen, X., Villanueva, F.S., 2012. Ultrasound-targeted microbubble destruction to deliver siRNA cancer therapy. *Cancer Res.* 72, 6191–6199. doi:<http://dx.doi.org/10.1158/0008-5472.CAN11-4079>.
- Choi, J.J., Selert, K., Vlachos, F., Wong, A., Konofagou, E.E., 2011. Noninvasive and localized neuronal delivery using short ultrasound pulsed and microbubbles. *Proc. Natl. Acad. Sci. U. S. A.* 108, 16539–16544. doi:<http://dx.doi.org/10.1073/pnas.1105116108>.
- Grainger, S.J., Serna, J.V., Sunny, S., Zhou, Y., Deng, C.X., El-Sayed, M.E.H., 2010. Pulsed ultrasound enhances nanoparticle penetration into breast cancer spheroids. *Mol. Pharm.* 7, 2006–2019. doi:<http://dx.doi.org/10.1021/mp100280b>.
- Hauff, P., Seemann, S., Reszka, R., Scultze-Mosgau, M., Reinhardt, M., Buzasi, T., Plath, T., Rosewicz, S., Schirner, M., 2005. Evaluation of gas-filled microparticles and

- sonoporation as gene delivery system: feasibility study in rodent tumor models. *Radiology* 236, 572–578. doi:<http://dx.doi.org/10.1148/radiol.2362040870>.
- Ingargiola, M., Runge, R., Heldt, J.M., Freudenberg, R., Steinbach, J., Cordes Baumann, N.M., Kotzerke, J., Brockhoff, G., Kunz-Schughart, L.A., 2014. Potential of a cetuximab-based radioimmunotherapy combined with external irradiation manifests in a 3-D cell assay. *Int. J. Cancer* 135, 968–980. doi:<http://dx.doi.org/10.1002/ijc.28735>.
- Komarova, Y., Malik, A.B., 2010. Regulation of endothelial permeability via paracellular and transcellular transport pathways. *Ann. Rev. Physiol.* 72, 463–493. doi:<http://dx.doi.org/10.1146/annurev-physiol-021909-135833>.
- Kyle, A.H., Huxham, L.A., Chiam, A.S.J., Sim, D.H., Minchinton, A.I., 2004. Direct assessment of drug penetration into tissue using a novel application of three-dimensional cell culture. *Cancer Res.* 64, 6304–6309. doi:<http://dx.doi.org/10.1158/0008-5472.CAN-04-1099>.
- Kyle, A.H., Huxham, L.A., Yeoman, D.M., Minchinton, A.I., 2007. Limited tissue penetration of taxanes: a mechanism for resistance in solid tumors. *Cancer Res.* 13, 2804–2810. doi:<http://dx.doi.org/10.1158/1078-0432.CCR-06-1941>.
- Lentacker, I., de Cock, I., Deckers, R., de Smidt, S.C., Moonen, C.T.W., 2014. Understanding ultrasound induced sonoporation: definitions and underlying mechanisms. *Adv. Drug Deliv. Rev.* 72, 49–64. doi:<http://dx.doi.org/10.1016/j.addr.2013.11.008>.
- Manzoor, A.A., Lindner, L.H., Landon, C.D., Park, J.Y., Simnick, A.J., Dreher, M.R., Das, S., Hanna, G., Park, W., Chilkoti, A., Koning, G.A., ten Hagen, T.L.M., Needham, D., Dewhurst, M.W., 2012. Overcoming limitations in nanoparticle drug delivery: triggered, intravascular release to improve drug penetration into tumors. *Cancer Res.* 72, 5566–5575. doi:<http://dx.doi.org/10.1158/0008-5472.CAN-12-1683>.
- McMillin, D.W., Negri, J.M., Mitsiades, C.S., 2013. The role of tumour–stromal interactions in modifying drug response: challenges and opportunities. *Nat. Rev. Drug Discov.* 12, 217–228. doi:<http://dx.doi.org/10.1038/nrd3870>.
- Minchinton, A.I., Tannock, I.F., 2006. Drug penetration in solid tumors. *Nat. Rev. Cancer* 6, 583–592. doi:<http://dx.doi.org/10.1038/nrc1893>.
- Nhan, T., Burgess, A., Cho, E.E., Stefanovic, B., Lilge, L., Hynynen, K., 2013. Drug delivery to the brain by focused ultrasound induced blood–brain barrier disruption: quantitative evaluation of enhanced permeability of cerebral vasculature using two-photon microscopy. *J. Control. Release* 172, 274–280. doi:<http://dx.doi.org/10.1016/j.jconrel.2013.08.029>.
- Nishihara, H., 2014. Human pathological basis of blood vessels and stromal tissue for nanotechnology. *Adv. Drug Deliv. Rev.* doi:<http://dx.doi.org/10.1016/j.addr.2014.01.005> in press.
- Primeau, A.J., Rendon, A., Hedley, D., Lilge, L., Tannock, I.F., 2005. The distribution of the anticancer drug doxorubicin in relation to blood vessels in solid tumors. *Clin. Cancer Res.* 11, 8782–8788. doi:<http://dx.doi.org/10.1158/1078-0432.CCR-05-1664>.
- Sagnella, S.M., Duong, H., MacMillan, A., Boyer, C., Whan, R., McCarroll, J.A., Davis, T. P., Kavallaris, M., 2014. Dextran-based doxorubicin nanocarriers with improved tumor penetration. *Biomacromolecules* 15, 262–275. doi:<http://dx.doi.org/10.1021/bm401526d>.
- Tinkov, S., Coester, C., Serba, S., Geis, N.A., Katus, H.A., Winter, G., Bekereldjian, R., 2010. New doxorubicin-loaded phospholipid microbubbles for targeted tumor therapy: in-vivo characterization. *J. Control. Release* 148, 368–372. doi:<http://dx.doi.org/10.1016/j.jconrel.2010.09.004>.